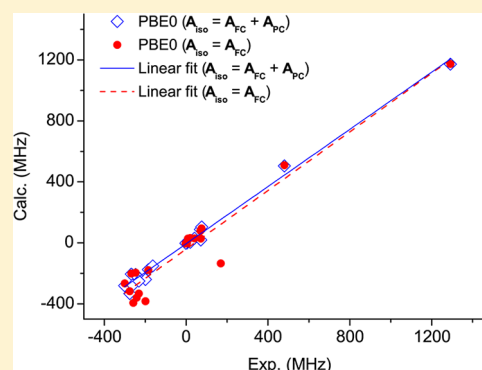


# Validating and Analyzing EPR Hyperfine Coupling Constants with Density Functional Theory

Erik D. Hedegård,<sup>\*,†</sup> Jacob Kongsted,<sup>†</sup> and Stephan P. A. Sauer<sup>‡</sup><sup>†</sup>Department of Physics, Chemistry and Pharmacy, University of Southern Denmark<sup>‡</sup>Department of Chemistry, University of University, Copenhagen

## S Supporting Information

**ABSTRACT:** This paper focuses on the calculation of the (isotropic) hyperfine coupling tensor,  $A_{\text{iso}}^K$ , which consists of the Fermi contact term ( $A_{\text{FC}}^K$ ) and a spin orbit correction, the pseudocontact term ( $A_{\text{PC}}^K$ ). Using the aug-cc-pVTZ-J basis set, we test a range of correlation exchange functionals against experimental values for a series of first row transition metal complexes. This has been done both with ( $A_{\text{iso}}^K = A_{\text{FC}}^K + A_{\text{PC}}^K$ ) and without ( $A_{\text{iso}}^K = A_{\text{FC}}^K$ ) spin orbit coupling included. Overall, hybrid functionals perform best, although some exceptions are found. Furthermore, we analyze molecular orbital contributions to the Fermi contact term. We find a great difference in the relative magnitude of contributions from frontier orbitals and inner or outer-core orbitals. Complexes, where the frontier orbital contribution exceeds the core-orbital contributions, are always small, ionic complexes ("class 1"). For these complexes, the computational requirements with respect to the one-electron basis set are not severe, and regular basis sets such as aug-cc-pVTZ provide reasonable results. Unfortunately, the core contributions to  $A_{\text{FC}}^K$  are either comparable ("class 2") or far exceed ("class 3") the contributions from the frontier orbitals in both organometallic and traditional coordination complexes. Agreement with experimental results can for these complexes only be obtained by use of specialized core-property basis sets such as the aug-cc-pVTZ-J basis set.



## 1. INTRODUCTION

Investigation and characterization of inorganic coordination complexes with d-block metals rely to a large degree on their magnetic properties. The magnetic properties of a given compound can provide even structural information which becomes valuable in the absence of an X-ray structure. For compounds with nonzero spin, Electron Paramagnetic Resonance (EPR) is in this respect a central spectroscopic technique<sup>1</sup> which is still under rapid development. This has led to an ever wider range of applications notably within bioinorganic chemistry,<sup>2–9</sup> where EPR holds great promise for structure elucidation of intermediates and investigation of mechanisms in enzyme catalysts. Elaborate fitting procedures for the so-called spin-Hamiltonian

$$\hat{H}_{\text{spin}} = \mu_B \mathbf{g} \hat{\mathbf{S}} \mathbf{B} + \sum_K \hat{\mathbf{S}} \mathbf{A}^K \hat{\mathbf{I}}^K + D \left[ \hat{S}_z^2 - \frac{1}{3} S(S+1) \right] + E [\hat{S}_x^2 - \hat{S}_y^2] \quad (1)$$

have been devised to extract meaningful quantities from the measured spectra. The  $\mathbf{g}$  tensor, the hyperfine coupling (HFC) tensor for nucleus  $K$ ,  $\mathbf{A}^K$ , and the zero-field splitting constants,  $D$  and  $E$  (enter for  $S > 1/2$  systems), are thus all obtained as fitting constants. We focus here on the hyperfine coupling (HFC) tensor, which provides the important structural information about the coordination environment of the spin

center. While obtained as a fitting constant in eq 1, the HFC tensor is composed of the contributions

$$\mathbf{A}^K = \mathbf{A}_{\text{iso}}^K + \mathbf{A}_{\text{SD}}^K \quad (2)$$

which can be calculated from first principles calculations. The first term in eq 2 is an isotropic tensor which depends on the spin density at nucleus  $K$ , while the second term is an anisotropic, trace-less  $3 \times 3$  magnetic dipole tensor, called the spin-dipolar tensor. Without spin orbit coupling, the isotropic term is identical to the "Fermi-contact" term,  $A_{\text{FC}}^K$ , whereas spin orbit coupling introduces an additional term known as the "pseudo-contact" term,  $A_{\text{PC}}^K$

$$\mathbf{A}_{\text{iso}}^K = \mathbf{A}_{\text{FC}}^K + \mathbf{A}_{\text{PC}}^K \quad (3)$$

The pseudocontact term can be evaluated by several procedures.<sup>10,11</sup> Corrections due to spin orbit coupling on the spin-dipolar term also exists and have been implemented. However, these will not be considered here, since the  $\mathbf{A}_{\text{iso}}^K$  term usually exceeds the  $\mathbf{A}_{\text{SD}}^K$  contribution by far and is the most challenging to obtain accurately.<sup>12–18</sup> For d-block complexes, the system size often makes highly correlated wave function calculations prohibitive, and apart from a few studies on small systems,<sup>19</sup> most studies apply density functional theory. Several

Received: March 5, 2013

Published: April 15, 2013

benchmark studies have tested a wide range of different functionals for HFCs.<sup>12,16</sup> A general feature of these benchmarks has been that they have compiled the underlying basis sets from a number of different sources. This prompted us to construct a unified basis set for the 3d row,<sup>20</sup> using the same philosophy as the aug-cc-pVTZ-J basis set devised for NMR J-coupling constants.<sup>21,22</sup> These basis sets were subsequently benchmarked, showing that they were close to basis set saturation at significant reduced cost.<sup>23</sup> They also gave substantial improvement over the aug-cc-pVTZ and aug-cc-pCVTZ basis sets when compared to experimental results. However, an important factor which was not considered in our previous studies is the effect of spin orbit coupling.<sup>10,24–26</sup> In this paper, we benchmark the performance of several functionals in calculations of  $A_{\text{FC}}^{\text{K}}$  using the aug-cc-pVTZ-J basis sets and including the pseudo-contact term. The test set is similar to the one used in our previous studies and is accordingly varied both in terms of metal ligation and metals involved. We further investigate the effect of including exact exchange into the functionals on  $A_{\text{FC}}^{\text{K}}$ . In this part, we follow the work of Kaupp and co-workers<sup>27–30</sup> using a decomposition of the  $A_{\text{iso}}^{\text{K}}$  tensor into molecular orbital contributions. Unexpectedly, we found that such a decomposition can also explain the large difference in importance of using basis sets with flexible core regions among different classes of coordination complexes.

## 2. COMPUTATIONAL METHOD

**2.1. Test Set of Molecules.** The test set is comprised of 21 molecules (see Table 1) containing 3d metals. For the geometry optimization, we use the same specifications as described in our previous studies.<sup>20,23</sup> The first series of molecules in Table 1 (1–3) are small molecules, which are of mainly ionic character, while 7 and 8 are organometallic complexes. The molecules 9–21 are more traditional

**Table 1. Test Set of Molecules Employed in This Study and Measured Values of Their Hyperfine Coupling Constants**

molecules	index	symmetry <sup>a</sup>	exptl. (MHz)
MnO	1	$C_{\infty v}$	480 <sup>31</sup>
ZnF	2	$C_{\infty v}$	1291.3 <sup>32</sup>
TiF <sub>3</sub>	3	$D_{3h}$	−185 <sup>33</sup>
Mn(CO) <sub>5</sub>	4	$C_{4v}$	6 <sup>34</sup>
[Fe(CO) <sub>5</sub> ] <sup>+</sup>	5	$C_{4v}$	−2 <sup>35</sup>
Ni(CO) <sub>3</sub> H	6	$C_{3v}$	9.0 <sup>36</sup>
[Cr(CO) <sub>4</sub> ] <sup>+</sup>	7	$T_h$	42 <sup>37</sup>
Cu(CO) <sub>3</sub>	8	$D_{3h}$	71.05 <sup>38</sup>
[V(H <sub>2</sub> O) <sub>6</sub> ] <sup>2+</sup>	9	$O_h$	−247 <sup>b</sup>
[Mn(H <sub>2</sub> O) <sub>6</sub> ] <sup>2+</sup>	10	$O_h$	−245 <sup>39</sup>
[Cr(NO)(H <sub>2</sub> O) <sub>5</sub> ] <sup>2+</sup>	11	$C_{4v}$	70.15 <sup>40</sup>
[Cr(NS)(H <sub>2</sub> O) <sub>5</sub> ] <sup>2+</sup>	12	$C_{4v}$	75.85 <sup>40</sup>
Cu(acac) <sub>2</sub>	13	$D_{4h}$	−223.33 <sup>41</sup>
[Cu(en) <sub>2</sub> ] <sup>2+</sup>	14	$D_{4h}$	−258 <sup>42</sup>
[Cu(NH <sub>3</sub> ) <sub>4</sub> ] <sup>2+</sup>	15	$D_{2d}$	−242.67 <sup>42</sup>
V(O)(acac) <sub>2</sub>	16	$C_{4v}$	−307 <sup>43</sup>
Cr(N)(acac) <sub>2</sub>	17	$C_{4v}$	84.01 <sup>44</sup>
[Mn(N)(CN) <sub>4</sub> ] <sup>−</sup>	18	$C_{4v}$	−275.71 <sup>45</sup>
V(S <sub>2</sub> C <sub>2</sub> H <sub>2</sub> ) <sub>3</sub>	19	$D_{3h}$	−163 <sup>46</sup>
[Ni(mnt) <sub>2</sub> ] <sup>−</sup>	20	$D_{4h}$	20 <sup>47</sup>
Cu(Me <sub>2</sub> dte) <sub>2</sub>	21	$D_{4h}$	−236 <sup>48</sup>

<sup>a</sup>For 9–17 and 20 and 21, only approximate symmetry. <sup>b</sup>Taken from the compilation of Kossmann et al.<sup>16</sup>

coordination compounds. We have further subdivided the last set into three sets, where 9–15 are metals of “normal” oxidation states. [[Cr(NO)(H<sub>2</sub>O)<sub>5</sub>]<sup>2+</sup> and [Cr(NS)(H<sub>2</sub>O)<sub>5</sub>]<sup>2+</sup> are classified as “normal” oxidation states, although they are somewhat special due to the well-known ambiguity with assigning oxidation states in nitrosyl and thionitrosyl complexes; in the Enemark–Feltham notation, they would be classified as {CrNO}<sup>6</sup> and {CrNS}<sup>6</sup>, respectively. The set 16–18 contains metals in high oxidation states and 19–21 are S-coordinated.

**2.2. Calculation of Hyperfine Couplings.** All calculations of hyperfine couplings were performed with the ORCA program<sup>49</sup> at the DFT level of theory. This program allows the hyperfine coupling constant to be split into contributions from the molecular orbitals (MOs). The integration grid was always kept very large throughout (IntAcc = 6 and AngularGrid = 7) to ensure that the core density was correctly described. Seven exchange-correlation functionals were employed, namely the GGA functionals BLYP,<sup>50,51</sup> B3LYP,<sup>52,51</sup> PBE,<sup>53,54</sup> and PBE0;<sup>53,54</sup> the meta-GGA functionals TPSS<sup>55</sup> and TPSSH,<sup>55</sup> and the double hybrid functional B2PLYP.<sup>56</sup> B2PLYP is excluded here as its large content of exact exchange often leads to deterioration, and BP86 is not considered as the results for it are similar to the BLYP results. For each of the functionals, we use the aug-cc-pVDZ basis set for all atoms not directly attached to the metal. For the metal and the first coordination sphere, the core-correlation aug-cc-pCVTZ<sup>57</sup> or the core property aug-cc-pVTZ-J basis sets<sup>21,22,58–64</sup> are used. In the special case of  $\pi$ -back bonding diatomic ligands such as NO or CN<sup>−</sup>, both atoms are considered as first coordination sphere and are assigned the same basis set types. As a reference calculation, also the original aug-cc-pVTZ<sup>65–69</sup> basis set has been used for the metal and first coordination sphere. For each of the subsets of molecules in Table 1, the sections below only discuss representative examples, although all results have been compiled in the Supporting Information. For clarity, figures comparing MO contributions to  $A_{\text{FC}}^{\text{K}}$  obtained with different functionals will only include the orbitals where the *functionals* differ significantly, while figures comparing basis sets will have all significant contributions included. The former figures are always presented with the aug-cc-pVTZ-J results while the latter figures are always presented with results from the TPSSH functional. The experimental value for  $A_{\text{iso}}^{\text{K}}$  is shown in Figures 2–6 for comparison, but note that the calculated HFCs are *without* spin orbit correction and thus *not* representative for the performance of the functional.

## 3. RESULTS AND DISCUSSION

In previous work, we have established that calculations with the aug-cc-pVTZ-J basis sets are essentially free of basis set errors.<sup>20,23</sup> This facilitates the comparison between DFT calculations with different functionals and experimental results, since the functionals can no longer benefit from fortuitous error cancellation due to an incomplete basis set. It should be noted that the aug-cc-pVTZ-J basis set's convergence with respect to the  $A_{\text{FC}}^{\text{K}}$  term was not tested, but a basis set augmented with diffuse functions and of triple- $\zeta$  quality is expected to be close to the converged result for this term as well.

**3.1. Overall Functional Performance.** The results of a linear regression analysis for the correlation between calculated and experimental values of the hyperfine coupling constant for molecules 1–21 are given in Table 2 together with mean deviations from the experimental values. Results and fits for two

**Table 2.** Mean Absolute Deviation (MAD) and Mean Deviation from Experimental Values for Calculations with Different Functionals and the aug-cc-pVTZ-J Basis Set on the Molecules 1–21 and Parameters for a Linear Regression Fit ( $y = ax + b$ ) of the Correlation between Calculated and Measured Values

functional	MAD (MHz)	mean deviation (MHz)	$a$	$R^2$
nonrelativistic ( $A_{\text{iso}} = A_{\text{FC}}$ )				
BLYP	55.94	16.56	0.8689 (0.052)	0.9351
B3LYP	50.59	−7.13	0.9367 (0.056)	0.9362
PBE	47.27	7.22	0.8772 (0.048)	0.9450
PBE0	51.83	−24.28	0.9616 (0.060)	0.9317
TPSS	43.81	6.15	0.8962 (0.051)	0.9426
TPSSh	42.54	−6.31	0.9270 (0.089)	0.9408
spin orbit corrected ( $A_{\text{iso}} = A_{\text{FC}} + A_{\text{PC}}$ )				
BLYP	64.44	28.66	0.8577 (0.035)	0.9689
B3LYP	34.22	14.54	0.9161 (0.024)	0.9866
PBE	52.45	21.01	0.8637 (0.021)	0.9809
PBE <sub>0</sub>	28.97	−4.91	0.9382 (0.022)	0.9900
TPSS	45.58	17.62	0.8884 (0.022)	0.9846
TPSSh	31.53	7.35	0.9156 (0.020)	0.9907

selected functionals are shown in Figure 1. Similar fits have also been performed using aug-cc-pVTZ and aug-cc-pCVTZ basis sets. As expected, the aug-cc-pVTZ-J basis set leads to a significantly improved correlation with experimental values, compared to aug-cc-pCVTZ and aug-cc-pVTZ (not shown). In terms of functional performance, it is first noted that inclusion of exact exchange in general improves the fit, both with and without spin–orbit corrections. We find that PBE0 provides overall the best fit and, upon inclusion of spin orbital coupling, also the lowest MAD. It has previously been suggested that functionals incorporating a large degree of exact exchange are beneficial in HFC calculations, especially when spin–orbit effects are included.<sup>10,24</sup> Our results here using the aug-cc-pVTZ-J basis set confirm these earlier studies. While the fits in Figure 1 and the statistical parameters in Table 2 give a broad overview, we have also investigated the three classes of molecules individually, using the MO contributions to the  $A_{\text{FC}}^{\text{K}}$  tensor. This analysis has been performed both to compare GGA and hybrid functionals and to investigate a peculiar observation, namely that the chemical nature of the compound under investigation seems to have a great impact on whether

specialized bases are required for a reasonable correspondence between theory and experiment or not.

**3.1.1. Small, Ionic Compounds.** First, the group of ionic transition metal compounds 1–3 is considered, using  $\text{TiF}_3$  as a representative example. The same conclusions can be drawn from the two linear molecules  $\text{MnO}$  and  $\text{ZnF}$ . Including exact Hartree–Fock exchange into the functionals leads for the molecules 1–3 to a small improvement with respect to the experimental values. These three molecules are completely dominated by  $A_{\text{FC}}^{\text{K}}$ , and corrections from the pseudocontact term are small. A comparison between the contributing orbitals to  $A_{\text{FC}}^{\text{Ti}}$  using TPSS and TPSSh functionals is given in Figure 2a. Similar conclusions are reached by comparing the other pairs of hybrid and nonhybrid functionals. The contributions to  $A_{\text{FC}}^{\text{Ti}}$  are found to be from either orbitals in the valence region (“frontier orbitals”) or orbitals buried in the core region. A closer analysis shows the core orbitals to be of mainly metal 2s and 3s character, which is in fine accordance with the detailed analysis given by Kaupp and Munzarová.<sup>12</sup> The frontier MOs which contribute to  $A_{\text{FC}}^{\text{Ti}}$  are mainly of metal 4s and ligand or 4s and metal 3d orbital character. A first glance at the results of the hybrid functionals seems to indicate that the pair of spin–orbitals 15 is responsible for a large negative contribution and the pair of spin–orbitals 17 for an even larger positive contribution quite contrary to the GGA functionals. A closer analysis of this “artificial spin-polarization” shows that for TPSSh the 15- $\alpha$  and 17- $\beta$  spin–orbitals are very similar despite their slight difference in orbital energy. These two orbitals should therefore be treated as a pair, while 15- $\beta$  correlates with 16- $\alpha$  and so forth. We have encountered this situation frequently, also in the other classes of investigated molecules, and both for hybrid and GGA functionals. This should be taken as a warning that this type of molecular orbital analysis requires a careful (graphical) investigation of each orbital or alternatively the use an overlap selection criterion.<sup>29</sup> In all figures, the focus has thus been on the contributions from corresponding  $\alpha$ - and  $\beta$ -spin pairs, although the frontier orbitals giving rise to “artificial spin polarization” or large contributions to  $A_{\text{FC}}^{\text{K}}$  will be plotted, as done in Figure 2. What differentiates compounds 1–3 from 4–21 is that the contribution from MOs of mixed 4s and 3d character in 1–3 is substantially larger than the contributions from both the core and the remaining valence MOs. This prompted us to investigate whether this might explain the very small effect of using aug-cc-pVTZ-J rather than aug-cc-pCVTZ

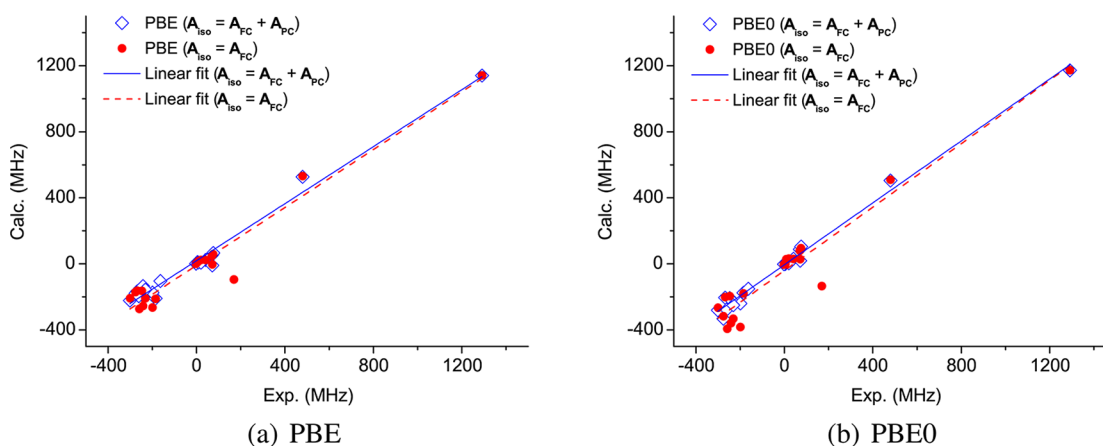


**Figure 1.** Correlation between calculated and experimental  $A_{\text{iso}}^{\text{K}}$  results with and without spin orbit corrections. Linear fits are also shown.

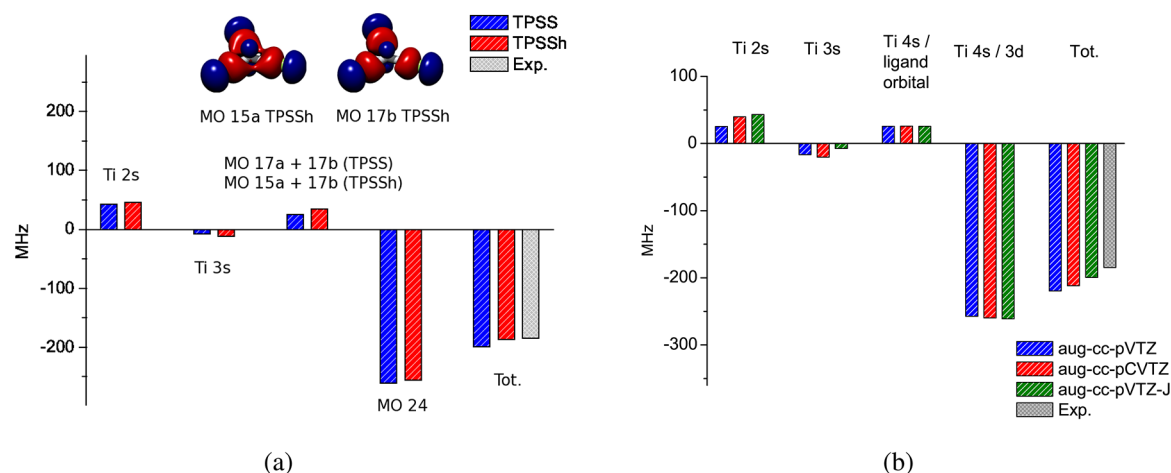


**Figure 2.** Contributions from molecular orbitals to  $A_{FC}^{Ti}$  in  $TiF_3$ . (a) Comparison between calculations with the TPSS and TPSSh functionals. (b) Comparison between calculations with the aug-cc-pVTZ, aug-cc-pCVTZ, and aug-cc-pVTZ-J basis sets.

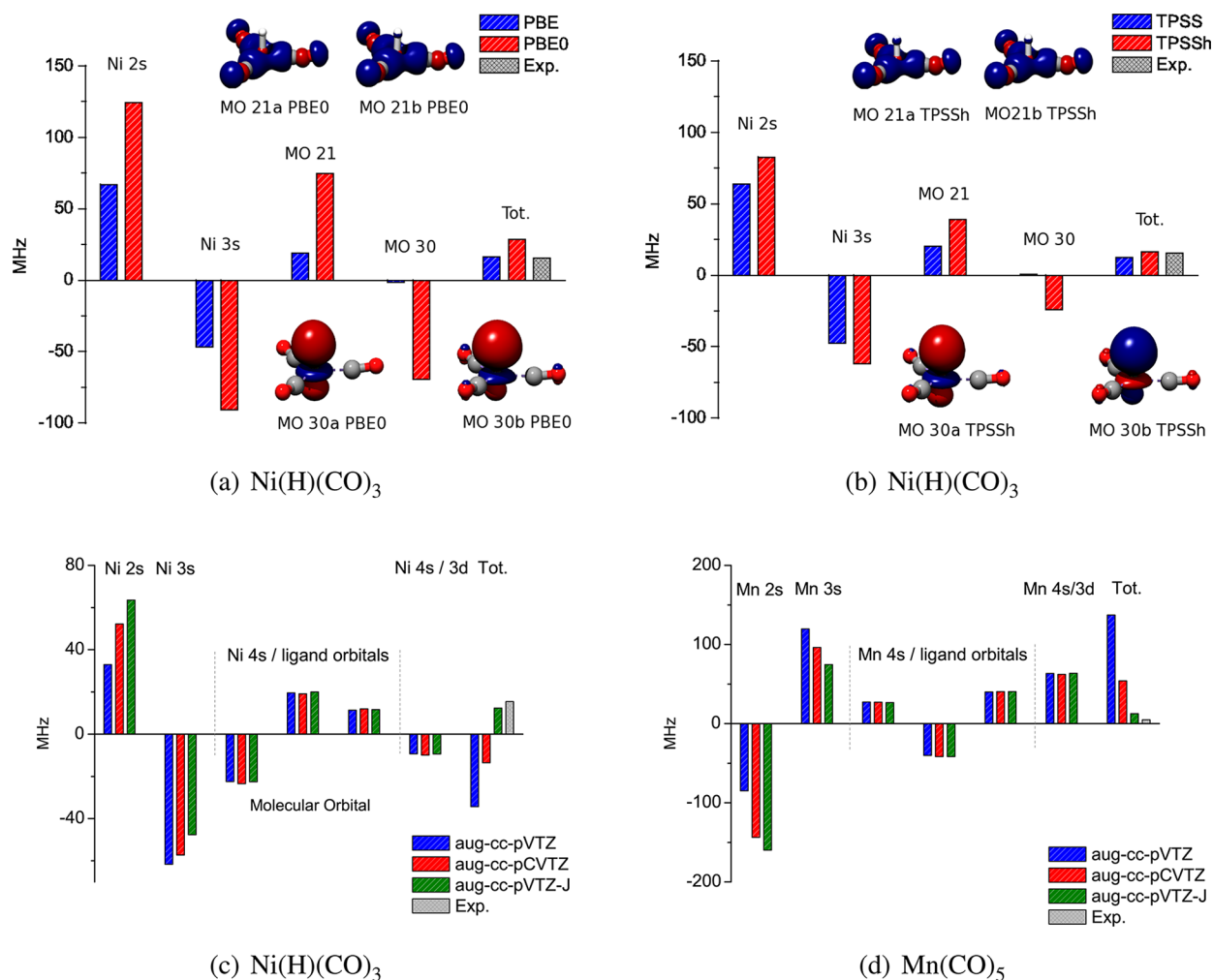


**Figure 3.** Contributions from molecular orbitals to  $A_{FC}^K$  in  $Ni(H)(CO)_3$  (a–c) and  $Mn(CO)_5$  (d). (a) Comparison between calculations with the PBE and PBE0 functionals. (b) Comparison between calculations with the TPSS and TPSSh functionals. (c) Comparison between calculations with the aug-cc-pVTZ, aug-cc-pCVTZ, and aug-cc-pVTZ-J basis sets. (d) Comparison between calculations with the aug-cc-pVTZ, aug-cc-pCVTZ, and aug-cc-pVTZ-J basis sets.

or aug-cc-pVTZ basis sets, since the three basis sets are likely to yield similar values for the contributions for the frontier orbitals. Figure 2b confirms that the three basis sets differ significantly in the core region, but the differences for the total

$A_{FC}^K$  value are drowned in the large contribution from the valence orbitals, where the three basis sets indeed are in close agreement. Thus, for molecules where the contributions from frontier orbitals dominate the total  $A_{FC}^K$  tensor, regular basis sets



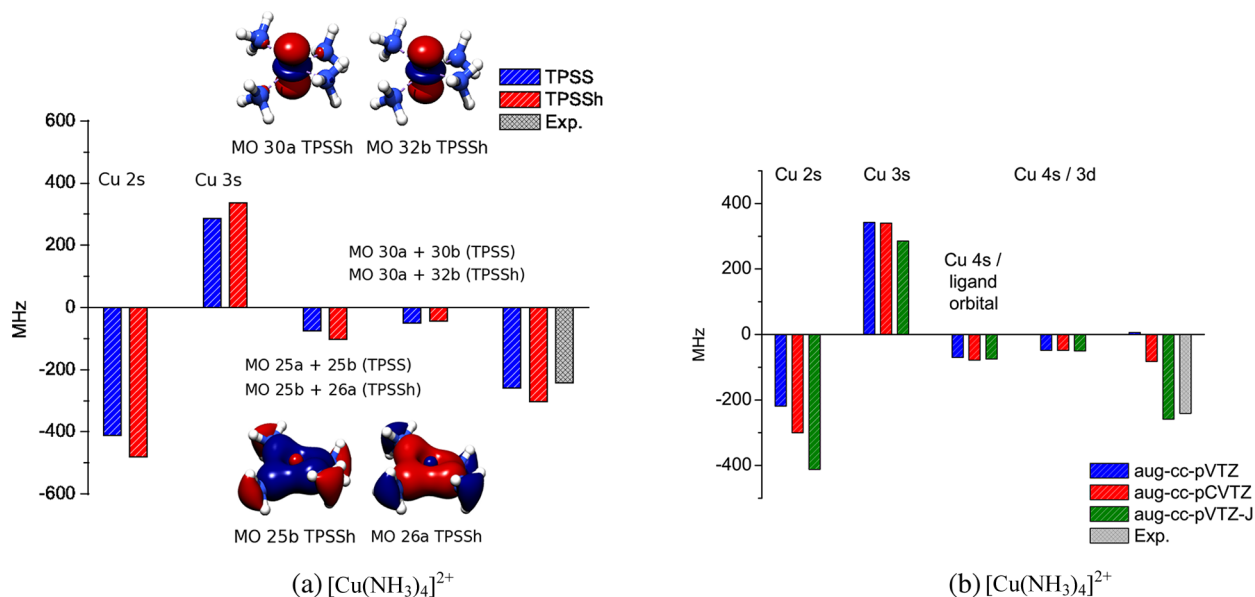


**Figure 4.** Contributions from molecular orbitals to  $A_{FC}^{Cu}$  in  $[Cu(NH_3)_4]^{2+}$ . (a) Comparison between calculations with the TPSS and TPSSh functionals. (b) Comparison between calculations with the aug-cc-pVTZ, aug-cc-pCVTZ, and aug-cc-pVTZ-J basis sets.

such as aug-cc-pVTZ can give reasonable results. We henceforth denote this class of molecules “class 1.” We note that the importance of spin polarization contributions to  $A_{FC}^{K}$  from the valence shell has been discussed for copper complexes by Remenyi et al.<sup>29</sup>

**3.1.2. Organometallic Complexes.** The organometallic complexes 4–8 are more varied with respect to functional performance than the small ionic molecules. A further complication is that while spin–orbit coupling effects are rather small for the isoelectronic  $Mn(CO)_5$  and  $[Fe(CO)_5]^+$ , they are large in  $Ni(H)(CO)_3$  and  $Cu(CO)_3$ , and for these two molecules the functional performance cannot be addressed before considering the pseudocontact term. It should be mentioned that the small absolute value of the HFC tensors in  $Mn(CO)_5$  and  $[Fe(CO)_5]^+$  also has the effect of making spin orbit coupling important. We thus postpone the discussion of the best performing functional and mainly discuss the difference between GGA and hybrid functionals along with the difference between basis sets, using the orbital contributions to  $A_{FC}^{K}$ . For this discussion, we use  $Ni(H)(CO)_3$  and  $Mn(CO)_5$  as examples. The MO contributions to  $A_{FC}^{Ni}$ , which differ most between nonhybrid and hybrid functionals, are shown in Figure 3a and b for the PBE/PBE0 and TPSS/TPSSh pairs, respectively. From these figures, it is evident that introducing exact exchange into the functional leads to large differences in contributions to  $A_{FC}^{K}$  from metal core orbitals, 2s and 3s. This is not confined to core orbitals as the frontier MOs also give very different contributions, depending on whether the functional contains exact exchange or not. The effect is generally smaller for the *meta*-GGA, which might be caused by the smaller percentage of exact exchange in this functional (PBE0 contains 25% while TPSSh only 10%). The organometallic complexes 4–8 generally have contributions from core orbitals which exceed contributions from valence orbitals in size. As shown in Figure 3c for  $Ni(H)(CO)_3$  and Figure 3d for  $Mn(CO)_5$ , this explains the necessity for using a basis set with a flexible core region, thus separating these molecules from the small ionic molecules from the previous subsection: The aug-cc-pCVTZ basis set significantly underestimates the contribution from the

metal 2s orbitals to  $A_{FC}^{K}$ , compared to aug-cc-pVTZ-J. Furthermore, aug-cc-pCVTZ overestimates the contribution to  $A_{FC}^{K}$  from the metal 3s orbitals, leading for  $Mn(CO)_5$  to significantly overestimated  $A_{FC}^{Mn}$  values, while for  $Ni(H)(CO)_3$ ,  $A_{FC}^{Ni}$  is obtained with the wrong sign. Note that for  $Ni(H)(CO)_3$ , the inclusion of  $A_{FC}^{Ni}$  will not improve this, seeing that we obtain a negative value for the pseudocontact term in this compound (cf. Supporting Information, Table 4).

**3.1.3. Classical “Werner Type” Coordination Complexes.** The class of “Werner type” coordination compounds is here represented by molecules 9–15. For the complexes 9–12, the spin orbit coupling term constitutes only a minor part of the total tensor, and the  $A_{FC}^{K}$  term thus dominates. For this term, inclusion of exact exchange generally improves the results for the chromium complexes and also for the hexaaqua complexes. However, the large percentage of exact exchange in PBE0 can lead to overestimation, as for instance seen in  $[Cr(NS)-(H_2O)_5]^{2+}$  (c.f., Supporting Information Tables 2 and 3). With respect to the copper complexes 13–15, spin–orbit coupling is crucial for accurate results and will determine the functional performance. Accordingly, discussion will for now be limited to the  $A_{FC}^{Cu}$  term, and the accuracy of the functionals with respect to the experimental value will be postponed until the next section. For the simple  $[Cu(NH_3)_4]^{2+}$  complex, a comparison between the MOs which contribute to  $A_{FC}^{Cu}$  for the *meta*-GGA TPSS and its hybrid counterpart, TPSSh, is given in Figure 4a. Although different frontier orbitals occasionally are involved, the same conclusions are drawn for the hexaaqua complexes and the rest of the copper complexes. Thus, the effect of exact exchange is primarily to increase the spin polarization of the 2s and 3s orbitals of metal character. In the case of  $[Cu(NH_3)_4]^{2+}$ , introducing exact exchange also introduces “artificial spin polarization” among the frontier orbitals, c.f., Figure 4a. The largest contributions to  $A_{FC}^{K}$  in the Werner type complexes are from the orbitals of metal 2s and 3s character. Accordingly, the final results for these molecules will be heavily dependent on how the core orbitals are treated in the employed basis set. Using again  $[Cu(NH_3)_4]^{2+}$  as an example, the comparison of different basis sets in Figure 4b shows that the aug-cc-pCVTZ

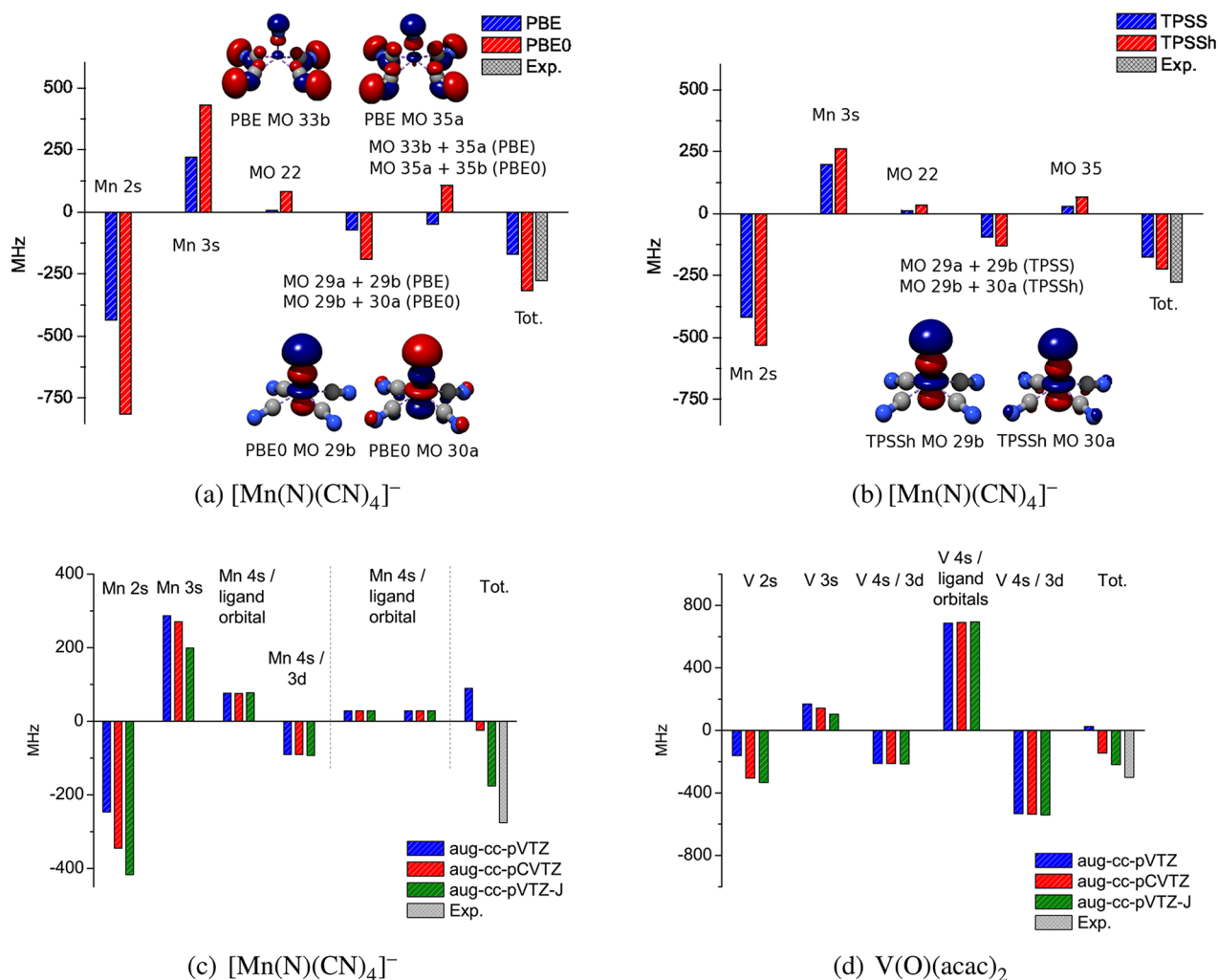


**Figure 5.** Contributions from molecular orbitals to  $A_{FC}^K$  in  $[\text{Mn}(\text{N})(\text{CN})_4]^-$  (a–c) and  $\text{V}(\text{O})(\text{acac})_2$  (d). (a) Comparison between calculations with the PBE and PBE0 functionals. (b) Comparison between calculations with the TPSS and TPSSh functionals. (c) Comparison between calculations with the aug-cc-pVTZ, aug-cc-pCVTZ, and aug-cc-pVTZ-J basis sets. (d) Comparison between calculations with the aug-cc-pVTZ, aug-cc-pCVTZ, and aug-cc-pVTZ-J basis sets.

basis set does not have a sufficiently flexible core region to describe  $A_{FC}^K$  in this type of molecule. It should be noted that we find one exception among the molecules 9–15, namely  $\text{Cu}(\text{acac})_2$  (13). Here, the contributions to  $A_{FC}^K$  from frontier orbitals are roughly similar to the contributions from core orbitals, and this molecule also shows less dependence on the applied basis set (although aug-cc-pVTZ-J is still to be recommended). We will denote 13 as “class 2,” while the remaining Werner type complexes will be referred to as “class 3.”

**3.1.4. High-Valent Coordination Compounds.** For the high-valent complexes investigated here, the pseudo-contact term ( $A_{FC}^K$ ) is small compared to  $A_{FC}^K$ , and the inclusion of exact exchange generally improves the comparison between calculated and experimental metal HFCs. The better agreement stems from the spin polarization in the metal 2s and 3s core orbitals, which is significantly enhanced by using hybrid functionals (especially for the PBE/PBE0 and BLYP/B3LYP pairs). However, an analysis of MO contributions to  $A_{FC}^K$  differs between GGA and their hybrid counterparts and the *meta*-GGA and hybrid *meta*-GGAs. For instance, in  $[\text{Mn}(\text{N})(\text{CN})_4]^-$ , cases of “artificial spin-polarization” are seen for both hybrid and nonhybrid GGA functionals. For the *meta*-GGA func-

tionals, only the hybrid functional leads to such cases. This is shown in Figure 5a,b. It should be noted that for  $[\text{Mn}(\text{N})(\text{CN})_4]^-$  (18) the hybrid functionals lead to spin contamination, especially for PBE0. However, we see no direct link between cases of “artificial spin polarization” and spin contamination. As an illustration, we note that for  $[\text{Mn}(\text{N})(\text{CN})_4]^-$ , the PBE functional does lead to “artificial spin polarization” with  $\langle \hat{S}^2 \rangle = 0.77$ , while TPSS does not, despite having almost the same value ( $\langle \hat{S}^2 \rangle = 0.78$ ). Likewise,  $\text{TiF}_3$  shows no sign of spin contamination, but nevertheless, “artificial spin polarization” occurs (c.f., Figure 2). Analyzing the MO contributions in the high-valent complexes 15–17 also leads to the conclusion that they show quite different behavior in how their molecular orbitals contribute to  $A_{FC}^K$ : While the isoelectronic systems  $\text{V}(\text{O})(\text{acac})_2$  (16) and  $\text{Cr}(\text{N})(\text{acac})_2$  (17) have large contributions from frontier orbitals, it is the opposite for  $[\text{Mn}(\text{N})(\text{CN})_4]^-$  (18) where the contributions from frontier orbitals are vanishingly small, c.f., Figure 5c,d. Thus, a balanced description of the metal orbitals of 2s and 3s character is of less importance in  $\text{V}(\text{O})(\text{acac})_2$  and  $\text{Cr}(\text{N})(\text{acac})_2$ , compared to  $[\text{Mn}(\text{N})(\text{CN})_4]^-$ . Consequently, the aug-cc-pCVTZ basis set performs reasonably well for  $\text{V}(\text{O})(\text{acac})_2$  and  $\text{Cr}(\text{N})(\text{acac})_2$ , while for  $[\text{Mn}(\text{N})(\text{CN})_4]^-$  these basis sets

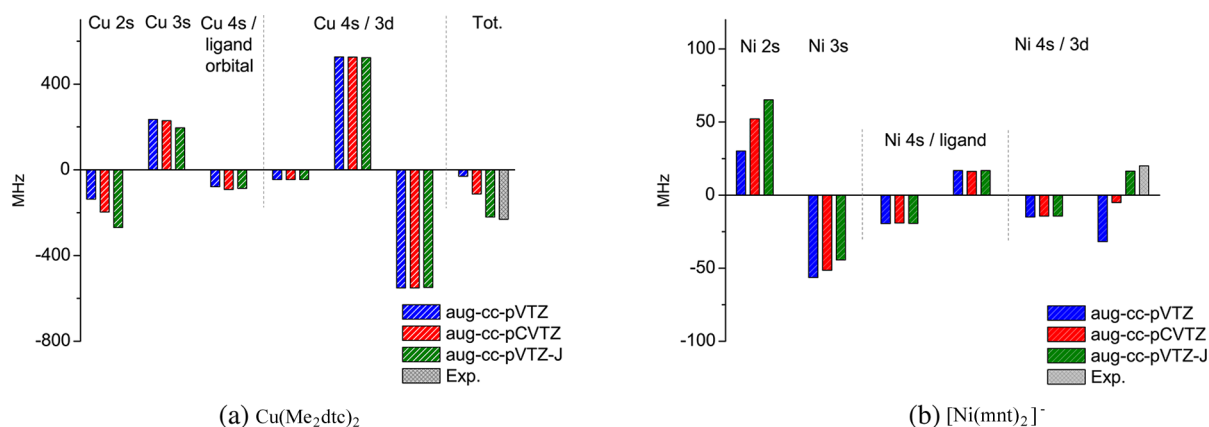


**Figure 6.** Contributions from molecular orbitals to  $A_{FC}^K$ . Comparison between calculations with the aug-cc-pVTZ, aug-cc-pCVTZ, and aug-cc-pVTZ-J basis sets and the TPSSH functional in (a)  $\text{Cu}(\text{Me}_2\text{dtc})_2$  and (b)  $[\text{Ni}(\text{mnt})_2]^-$ .

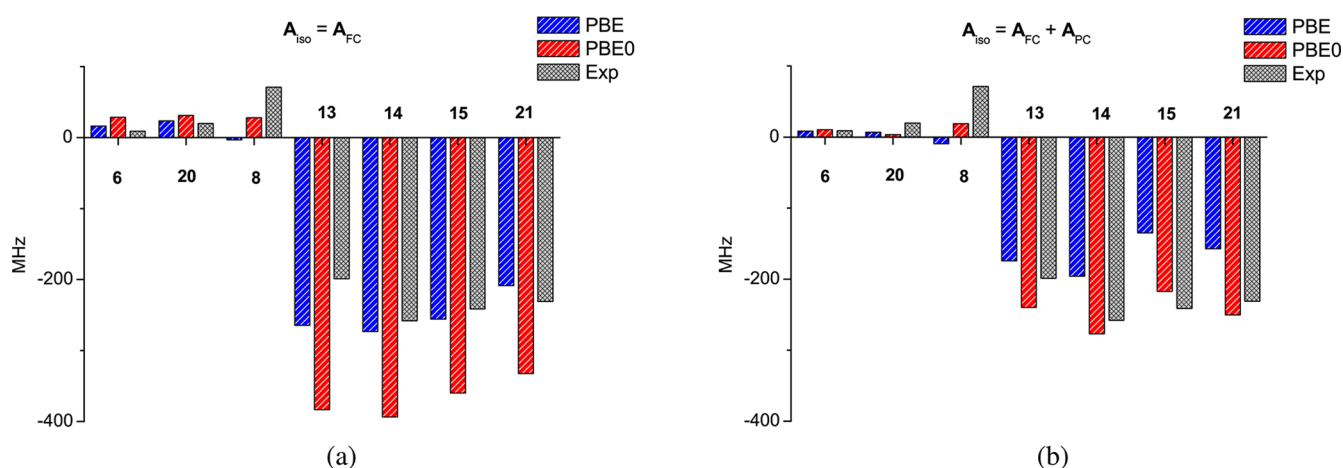


**Figure 7.** Comparison of experimental and calculated metal hyperfine coupling constants in Ni and Cu complexes, 6, 8, 13, 14, 15, 20, and 21, calculated with the PBE and PBE0 functionals and the aug-cc-pVTZ-J basis sets: (a) with  $A_{\text{iso}} = A_{FC}$  and (b) with  $A_{\text{iso}} = A_{FC} + A_{PC}$ .

lead to a severely underestimated  $A_{FC}^{\text{Mn}}$  value. Using the terminology from previous sections, we classify 16 and 17 as “class 2” and 18 as “class 3.”

**3.1.5. S-Coordinated Complexes.** The last molecules considered in this study are S-coordinated complexes 19–21. S-coordinated complexes behave in general similar to the regular complexes of “normal” oxidation states. As it was the case for the complexes 6, 8, and 13–15, also the S-coordinated complexes containing Ni or Cu have large contributions from the  $A_{PC}^K$  term. Accordingly, these will be discussed in the following subsection. Focusing on the  $A_{FC}^K$  term,  $\text{Cu}(\text{Me}_2\text{dtc})_2$  can with significant contributions from frontier orbitals be classified as “class 2” (see Figure 6). Thus, for this molecule, the aug-cc-pCVTZ basis set gives a reasonable estimate of  $A_{FC}^{\text{Cu}}$ . Interestingly, the Cu(II) coordination complexes with a first coordination sphere comprised of two row p-block atoms are all “class 3” and show much larger deviations between  $A_{FC}^{\text{Cu}}$  terms calculated with aug-cc-pCVTZ and aug-cc-pVTZ-J basis sets.  $[\text{Ni}(\text{mnt})_2]^-$  and  $\text{V}(\text{S}_2\text{C}_2\text{H}_2)_3$  (see Figure 6b for  $[\text{Ni}(\text{mnt})_2]^-$ ) both belong to “class 3” with contributions from the core orbitals dominating. Consequently, large discrepancies between aug-cc-pCVTZ and aug-cc-pVTZ-J for the calculated values of  $A_{FC}^K$  are to be expected (and are indeed observed).

**3.2. Importance of Spin Orbit Coupling.** For molecules containing Ni and Cu metals, 6, 8, 13–15, 20, and 21, it is

found that the spin orbit coupling contribution,  $A_{PC}^K$ , constitutes a significant part of  $A_{\text{iso}}^K$  and can occasionally determine which functional performs best. The calculated and experimental  $A_{\text{iso}}^K$  tensors are compiled in Figure 7a where  $A_{\text{iso}} = A_{FC}$  and Figure 7b where  $A_{\text{iso}} = A_{FC} + A_{PC}$ . The  $A_{FC}$  terms calculated with the nonhybrid functionals overestimate  $A_{\text{iso}}$  for these complexes, although two exceptions are  $\text{Cu}(\text{CO})_3$  (8) and  $\text{Cu}(\text{Me}_2\text{dtc})_2$  (21). Inclusion of exact exchange leads to increased spin polarization and thus to an increased  $A_{FC}$  term, which overestimates  $A_{\text{iso}}$  then even further.  $\text{Cu}(\text{CO})_3$  (8) is again an exception. Calculations of the  $A_{FC}$  term alone with the aug-cc-pVTZ-J basis sets and nonhybrid functionals lead therefore to results in better agreement with experimental results than with the hybrid functionals. However, the spin-orbit contribution  $A_{PC}^K$  has the opposite sign of the  $A_{FC}$  term, is relatively large, and is also increased in the hybrid functionals. This means that overall for these complexes, apart from  $[\text{Ni}(\text{mnt})_2]^-$  (20), the hybrid functionals give a better agreement between  $A_{FC} + A_{PC}$  and the experimental values for  $A_{\text{iso}}$ .

## 4. CONCLUSION

It has been investigated how the chemical nature of EPR active compounds influences the values of the metal isotropic hyperfine coupling tensor. This has been achieved by dividing the calculated  $A_{\text{iso}}^K$  values into contributions from molecular



orbitals of the compound in question. This analysis proved to be a powerful tool and has led to a classification of the transition metal complexes into three different classes: Complexes in “class 1” have frontier orbitals with much larger contributions to the HFC than from the metal 2s and 3s core orbitals. In “class 2,” the contributions from core orbitals are comparable to the frontier orbital contributions. Finally, in “class 3,” which is the largest class, core orbital contributions exceed by far the contributions from frontier orbitals. The three classes contain complexes of different oxidation states and ligand spheres, but “class 1” consists exclusively of small ionic molecules 1–3, whose HFCs can reasonably be calculated with standard basis sets like aug-cc-pVTZ. For “class 2” complexes, the hyperfine couplings calculated with the core–valence correlation basis set (aug-cc-pCVTZ) are not too far off from the experimental values, but use of a core-property basis set (here aug-cc-pVTZ-J) is still to be recommended. The regular aug-cc-pVTZ basis set, on the other hand, is not properly constructed for core properties and fails in calculations of  $A_{\text{iso}}^{\text{K}}$  apart from some extreme cases (“class 1 complexes”). The remaining complexes are of the “class 3” type, and the prevalence of “class 3” explains why the chosen basis set has on average great influence on HFC calculations. Inclusion of exact exchange into the functionals generally improves the agreement with the experimental HFCs, and we recommend PBE0 as a good compromise. The hybrid functionals perform better due to increased spin-polarization in the core metal 2s and 3s orbitals. However, we find some cases where frontier orbital spin-polarization can be of importance. For copper and nickel complexes, it is in addition central to include effects of spin orbit coupling as previously found by the groups of Kaupp and Neese.

## ■ ASSOCIATED CONTENT

### ● Supporting Information

Results for  $A_{\text{FC}}^{\text{K}}$  with the aug-cc-pCVTZ and aug-cc-pVTZ-J basis sets and results for  $A_{\text{iso}}^{\text{K}}$  and  $A_{\text{FC}}^{\text{K}}$  with the aug-cc-pVTZ-J basis set. This information is available free of charge via the Internet at <http://pubs.acs.org/>.

## ■ AUTHOR INFORMATION

### Corresponding Author

\*E-mail: [edh@sdu.dk](mailto:edh@sdu.dk).

### Notes

The authors declare no competing financial interest.

## ■ ACKNOWLEDGMENTS

This work has been supported by grants from the Danish Center for Scientific Computing (DCSC). J.K. thanks The Danish Councils for Independent Research (STENO and Sapere Aude programmes), the Lundbeck Foundation and the Villum Kann Rasmussen Foundation for financial support. E. D. H. thanks the OTICON and Augustines Funds for stipends.

## ■ REFERENCES

- (1) Bleaney, B.; Abragam, A. *Electron Paramagnetic Resonance of Transition Metal Ions*; Oxford University Press: New York, 1970; pp 133–209.
- (2) Mukhopadhyay, S.; Mandal, S. K.; Bhaduri, S. S.; Armstrong, W. H. *Chem. Rev.* **2004**, *104*, 3981.
- (3) Lubitz, W.; Reijerse, E.; van Gastel, M. *Chem. Rev.* **2007**, *107*, 4331–4365.
- (4) Dikanov, S. A.; Samoilova, R. I.; Kappl, R.; Crofts, A. R.; Hüttermann, J. *Phys. Chem. Chem. Phys.* **2009**, *11*, 6807–6819.
- (5) Silakov, A.; Wenk, B.; Reijerse, E.; Lubitz, W. *Phys. Chem. Chem. Phys.* **2009**, *11*, 6592–6599.
- (6) Davydov, R.; Kappl, R.; Hüttermann, J.; Peterson, J. A. *FEBS Lett.* **1991**, *295*, 113.
- (7) Davydov, R.; Makris, T. M.; Kofman, V.; Werst, D. E.; Sligar, S. G.; Hoffman, B. M. *J. Am. Chem. Soc.* **2001**, *123*, 1403.
- (8) Davydov, R.; Satterlee, J. D.; Fujii, H.; Sauer-Masarwa, A.; Busch, D. H.; Hoffman, B. M. *J. Am. Chem. Soc.* **2003**, *125*, 16340.
- (9) Davydov, R.; Perera, R.; Jin, S.; Yang, T.-C.; Bryson, T. A.; Sono, M.; Dawson, J. H.; Hoffman, B. M. *J. Am. Chem. Soc.* **2005**, *127*, 1403.
- (10) Neese, F. *J. Chem. Phys.* **2003**, *118*, 3939–2948.
- (11) Abuznikov, A. V.; Vaara, J.; Kaupp, M. *J. Chem. Phys.* **2004**, *120*, 2127–2139.
- (12) Munzarová, M.; Kaupp, M. *J. Phys. Chem. A* **1999**, *103*, 9966–9983.
- (13) Neese, F. *J. Phys. Chem. A* **2001**, *105*, 4290–4299.
- (14) Abuznikov, A. V.; Kaupp, M.; Malkin, V. G.; Reviakine, R.; Malkina, O. L. *Phys. Chem. Chem. Phys.* **2002**, *4*, 5467–5474.
- (15) Kaupp, M.; Bühl, M.; Malkin, V. G. *Calculation of NMR and EPR parameters. Theory and applications*; Wiley: New York, 2004; pp 463–483.
- (16) Kossmann, S.; Kirchner, B.; Neese, F. *Mol. Phys.* **2007**, *105*, 2049.
- (17) Neese, F. *Curr. Opin. Chem. Biol.* **2003**, *7*, 125–135.
- (18) Schöneboom, J. C.; Neese, F.; Thiel, W. *J. Am. Chem. Soc.* **2005**, *127*, 5840–5853.
- (19) Knight, L. B., Jr.; Babb, R.; Ray, M.; Banisaukas, T. J., III; Russon, L.; Dailey, S.; Davidson, E. R. *J. Chem. Phys.* **1996**, *105*, 10237–10250.
- (20) Hedegård, E. D.; Kongsted, J.; Sauer, S. P. A. *J. Chem. Theory Comput.* **2011**, *7*, 4077–4087.
- (21) Provasi, P. F.; Aucar, G. A.; Sauer, S. P. A. *J. Chem. Phys.* **2001**, *115*, 1324–1334.
- (22) Provasi, P. F.; Sauer, S. P. A. *J. Chem. Phys.* **2010**, *133*, 054308.
- (23) Hedegård, E. D.; Kongsted, J.; Sauer, S. P. A. *Phys. Chem. Chem. Phys.* **2012**, *14*, 10669–10676.
- (24) Remenyi, C.; Reviakine, R.; Abuznikov, A. V.; Vaara, J.; Kaupp, M. *J. Phys. Chem. A* **2004**, *108*, 5026–5033.
- (25) Fritscher, J.; Hrobárik, P.; Kaupp, M. *J. Phys. Chem. B* **2007**, *111*, 4616–4629.
- (26) Fritscher, J.; Hrobárik, P.; Kaupp, M. *Inorg. Chem.* **2007**, *46*, 8146.
- (27) Munzarová, M.; Kaupp, M. *J. Am. Chem. Soc.* **2000**, *122*, 11900–11913.
- (28) Remenyi, C.; Munzarová, M.; Kaupp, M. *J. Phys. Chem. B* **2005**, *109*, 4227–4233.
- (29) Remenyi, C.; Reviakine, R.; Kaupp, M. *J. Phys. Chem. A* **2006**, *110*, 4021–4033.
- (30) Remenyi, C.; Reviakine, R.; Kaupp, M. *J. Phys. Chem. B* **2007**, *111*, 8290–8304.
- (31) Namiki, K.; Saito, S. *J. Chem. Phys.* **1997**, *107*, 8848–8853.
- (32) Flory, M. A.; McLamarrah, S. K.; Ziurys, L. M. *J. Chem. Phys.* **2006**, *125*, 194304.
- (33) DeVore, T. C.; Weltner, W., Jr. *J. Am. Chem. Soc.* **1977**, *99*, 4700–4703.
- (34) Howard, J. A.; Morton, J. R.; Preston, K. F. *Chem. Phys. Lett.* **1981**, *83*, 226–228.
- (35) Lionel, T.; Morton, J. R.; Preston, K. F. *J. Chem. Phys.* **1982**, *76*, 234–239.
- (36) Morton, J. R.; Preston, K. F. *J. Chem. Phys.* **1984**, *81*, 5775–5778.
- (37) Fairhurst, S. A.; Morton, J. R.; Preston, K. F. *Chem. Phys. Lett.* **1984**, *104*, 112–114.
- (38) Kasai, P. H.; Jones, P. M. *J. Am. Chem. Soc.* **1985**, *107*, 813–818.
- (39) Upreti, G. C. *J. Magn. Reson.* **1974**, *14*, 274–278.
- (40) Dethlefsen, J. W.; Dössing, A. *Inorg. Chim. Acta* **2009**, *362*, 259–262.



- (41) Maki, A. H.; R., M. B. *J. Chem. Phys.* **1958**, *29*, 31–34.
- (42) Scholl, H.-J.; Hüttermann, J. *J. Phys. Chem.* **1992**, *96*, 9684–9691.
- (43) Dodge, R. P.; Templeton, D. H. *J. Phys. Chem.* **1980**, *84*, 2668.
- (44) Hedegård, E. D.; Schau-Magnussen, M.; Bendix, J. *Inorg. Chem. Commun.* **2011**, *14*, 719–721.
- (45) Bendix, J.; Meyer, K.; Weyhermüller, T.; Bill, E.; Metzler-Nolte, N.; Wieghardt, K. *Inorg. Chem.* **1998**, *37*, 1767–1775.
- (46) Kondo, M.; Minakoshi, S.; Iwata, K.; Shimizu, T.; Matsuzaka, H.; Kamigata, N.; Kitagawa, S. *Chem. Lett.* **1996**, 489–490.
- (47) Maki, A. H.; Edelstein, N.; Davison, A.; Holm, R. H. *J. Am. Chem. Soc.* **1964**, *86*, 4580–4587.
- (48) Ivanov, A. V.; Ivakhnenko, E. V.; Forsling, W.; Gerasimenko, A. V.; Bukvetskii, B. V. *Zh. Neorg. Khim.* **2002**, *47*, 468–480.
- (49) Neese, F. *ORCA - An ab initio, DFT and semiempirical SCF-MO package*; University of Bonn: Bonn, Germany, 2009.
- (50) Becke, A. D. *Phys. Rev. A* **1988**, *38*, 3098.
- (51) Lee, C.; Yang, W.; Parr, R. G. *Phys. Rev. B* **1988**, *37*, 785–789.
- (52) Becke, A. D. *J. Chem. Phys.* **1993**, *98*, 5648–5652.
- (53) Perdew, J. P.; Burke, K.; Wang, Y. *Phys. Rev. Lett.* **1996**, *77*, 3865–3868.
- (54) Perdew, J. P.; Burke, K.; Wang, Y. *Phys. Rev. Lett.* **1997**, *78*, 1396.
- (55) Tao, J.; Perdew, J. P.; Staroverov, G. E. *Phys. Rev. Lett.* **2003**, *91*, 146401–146401.
- (56) Grimme, S. *J. Chem. Phys.* **2006**, *124*, 034108.
- (57) Peterson, K. A.; Dunning, T. H., Jr. *J. Chem. Phys.* **2002**, *117*, 10548.
- (58) Enevoldsen, T.; Oddershede, J.; Sauer, S. P. A. *Theor. Chem. Acc.* **1998**, *100*, 275–284.
- (59) Sauer, S. P. A.; Raynes, W. T. *J. Chem. Phys.* **2000**, *113*, 3121–3129.
- (60) Sauer, S. P. A.; Raynes, W. T. *J. Chem. Phys.* **2001**, *114*, 9193.
- (61) Sauer, S. P. A.; Raynes, W. T.; Nicholls, R. A. *J. Chem. Phys.* **2001**, *115*, 5994–6006.
- (62) Barone, V.; Provasi, P. F.; Peralta, J. E.; Snyder, J. P.; Sauer, S. P. A.; Contreras, R. H. *J. Phys. Chem. A* **2003**, *107*, 4748–4754.
- (63) Sanchez, M.; Provasi, P. F.; Aucar, G. A.; Sauer, S. P. A. *Adv. Quantum Chem.* **2005**, *48*, 161–183.
- (64) Rusakov, Y. Y.; Krivdin, L. B.; Sauer, S. P. A.; Levanova, E. P.; Levkovskaya, G. G. *Magn. Reson. Chem.* **2010**, *48*, 633–637.
- (65) Dunning, T. H., Jr.; Hay, P. H. In *Methods of Electronic Structure Theory*; Schaefer, H. F., III, Ed.; Plenum Press: New York, 1977; pp 1–27.
- (66) Dunning, T. H., Jr. *J. Chem. Phys.* **1970**, *53*, 2823–2833.
- (67) Dunning, T. H., Jr. *J. Chem. Phys.* **1971**, *55*, 716–723.
- (68) Dunning, T. H., Jr. *J. Chem. Phys.* **1989**, *90*, 1007–1023.
- (69) Balabanov, N. B.; Peterson, K. A. *J. Chem. Phys.* **2005**, *123*, 64107.